X-711-71-259
PREPRINT

NASA TM X-65603

ON-BOARD SPACECRAFT OPTICAL DATA PROCESSING

AKRAM S. HUSAIN-ABIDI

JUNE 1971

GODDARD SPACE FLIGHT CENTER
GREENBELT, MARYLAND

Paper presented at National Aeronautics and Space Administration and Optical Society of Americas, "Conference on Holography and Optical Filtering" at Huntsville, Alabama

X-711-71-259

ON-BOARD SPACECRAFT OPTICAL DATA PROCESSING

A. S. Husain-Abidi
Electronics Division

June 1971

Goddard Space Flight Center
Greenbelt, Maryland

ON-BOARD SPACECRAFT OPTICAL

DATA PROCESSING

Akram S. Husain-Abidi
Research Associate of National Academy of Science,
Goddard Space Flight Center

ABSTRACT

Optical data processing techniques are very attractive for data processing where image type data, in particular, is present, (as optical systems have two degrees of freedom). The use of hybrid optical-digital systems for use on "Earth Resources" and "Planetary" spacecraft is being explored. Attributed an on-board spacecraft optical system must possess low power, ruggedness and absence of mechanical or photographic links.

With on-board satellite use in mind, a unique system has been desinged. The main features of the system are the use of off-axis parabolic mirror segments as collimating Fourier transforming and image reconstructing elements, and a Gallium Arsenide laser diode as a point source of coherent electromagnetic radiation. Performance of this system for generating Fourier transform relationship and spatial filtering are very encouraging.

ON-BOARD SPACECRAFT OPTICAL DATA PROCESSING

Earth resources satellites and the earth resources experiments on-board space stations will sense a very large number of images. According to a rough estimate the total rate of information may be as high as 10^{12} bits per second. In order to extract usable information from this enormous amount of data, we believe that optical data processing techniques are ideally suited since they have two degrees of freedom, (contrasted with the electronic techniques which have inherently only one degree of freedom). Optical techniques are extremely useful for the performance of linear mathematical operation such as spectral analysis, complex spatial filtering, matched filtering and auto and cross-correlation.

An on-board spacecraft optical data processing system will be very useful as it will allow transmission of only the processed data rather than the data itself, resulting in an enormous saving of transmitter bandwidth. The development of these techniques will also be useful for other NASA missions such as to Mars and Venus.

The published account of optical data processing techniques goes as far back as 1873 when Ernst Abbe demonstrated in his classical paper that the diffraction pattern in the focal plane of a lens has all the characteristics of a two dimensional Fourier transform of the light distribution in the input information. He also realized the spatial filtering phenomenon. Porter in 1906 following the Abbes's work reported the experimental evidence of spatial filtering by manuplating the diffraction pattern in the Fourier transform plane to enhance or suppress certain features of the input information. During the period of 1954 to 1964 a number of papers appeared in the literature and perhaps the most important of them was the one by O'Neill in 1956. It was shown in his paper that the optical analog of a number of electrical concepts such as edge-sharpening and detection of periodic and isolated signals in the presence of noise can conveniently be performed. The published work of Vandee Lugt in 1964 for recording techniques of complex spatial filters was largely responsible for a re-evaluation of optical data processing techniques.

Figure 1 illustrates the conventional configuration of an optical system normally used for coherent optical data processing. Light from a He-Ne laser radiating at 6328Å wavelength is brought to a point focus by a microscope objective. A pinhole is placed in this focal plane to eliminate laser beam noise and to exclude stray light. Another lens is placed a focal length away from this plane to collimate the laser light. The input information is then placed a focal length away from a converging lens. This lens in its focal plane produces the Fraunhofer diffraction pattern of the input information in two dimensions. This diffraction pattern has all the characteristics of a two dimensional Fourier transform of the light distribution in the input information. If an arbitrary function is introduced in the input plane, a two dimensional spectrum of that function can be obtained in the Fourier transform plane. Spatial frequency filtering can also be performed in Fourier transform plane by manuplating the diffraction pattern. If a complex spatial filter is placed in the Fourier transform plane, the system can be used for auto or cross-correlation purposes.

This optical system works well in the laboratory environment and the performance of this system for spectrum analysis, spatial and complex spatial filtering and auto or cross correlation purposes has been reported in the literature. Since our main aim is to process the data on-board spacecraft, this system has two main drawbacks. The first is the low efficiency and bulky He-Ne gas laser and the second is the axial symmetry of the optical system.

A solid state Ga As laser has been used to overcome the first drawback. This laser is at least 10,000 times better in efficiency and probably the same order of magnitude smaller in overall size. Besides in a Ga As laser system the microscopic lens and pinhole spatial filter is not required, resulting in the minimization of optical alignment problems.

To overcome the second problem paraboloidal mirror segments are used. It has been found that paraboloidal mirror segments not only overcomes the axial symmetry problems but have a number of significant advantages over lenses. Let us start by considering the problems associated with the lenses.

The quality and resolution of Fourier transform relationship in the focal plane of the lenses is very much affected by the lens aberrations and the optical refracting material. Among the aberrations the following three are primarily responsible for the degradation of Fourier relationship:

(i) Spherical aberration

(ii) Astigmatism

(iii) Coma.

Beside overcoming these aberrations the other severe problem is the choice of the proper optical material. For an ultra-high quality lens suitable for data processing, the optical material should be:

(i) Optically homogeneous to a very high degree. (It is very important that the refractive index of the lens be constant throughout the material.)

(ii) Free from thermal and mechanical strains.

(iii) Optically Isotropic (i. e. the index of refraction at any point must be constant regardless of the direction in which the radiation is passing the point.

Therefore, for a good optical system with lenses it is necessary to rectify all the aberrations and one should also cope with the selection of proper optical material. Both of these problems are extremely difficult to rectify and costs are astronomical.

The other two disadvantages are the front surface reflections which are unavoidable and the axial symmetry of the system, (i. e. the optical system with lenses cannot be folded and therefore is a problem for spacecraft purposes).

Let us now consider the paraboloidal mirror as a linear element in an optical data processing system. Referring to Figure 2, light rays entering from the right parallel to the Z-axis are reflected from the mirror and intersect the Z-axis at the focal point f. The relationship between the incident and reflected scalar light fields at any point in the (x, y, zo) plane can be described in terms of a transfer function, t (x, y, zo). For mirrors, (as well as for lenses) the transfer function is strictly a phase function, and we have

$$\begin{aligned} t(x, y, z_0) &= e^{[j\phi(x, y, z_0)]} \\ &= e^{[jk\Delta(x, y, z_0)]} \end{aligned} \tag{1}$$

The term ϕ (x, y, zo) is the phase difference in radians between the incident and reflected fields, k is the wave number $2\pi/\lambda$ and $\Delta(x, y, z_0)$ is the difference in path lengths between the incident and reflected waves.

Again referring to Figure 1, we see that the total path difference is

$$\Delta(x, y, z_0) = 2(z_0 - \Delta z) \tag{2}$$

(this assumes no ray bending to the left of the (x, y, zo) plane, analogous to the thin lens approximation in lens analysis).

Now from the equation for a paraboloid of revolution,

$$\Delta z = \frac{x^2 + y^2}{4f} \tag{3}$$

therefore

$$\begin{aligned} t(x, y, z_0) &= e^{[jk\Delta(x, y, z_0)]} \\ &= e^{[j2kz_0]}\, e^{-jk\left[\frac{x^2 + y^2}{2f}\right]} \end{aligned} \tag{4}$$

In the case of a spherical thin lens, if the paraxial approximation is made, i. e. we consider only light rays close to the lens axis, the transfer function is found to be:[4]

$$t(x, y, z_0) = e^{[jknz_0]}\, e^{-jk\left[\frac{x^2 + y^2}{2f}\right]} \tag{5}$$

Here n is the index of refraction of the lens material, and zo is the lens thickness along the optical axis. It is important to note that the focal length f of a lens is a function of the index of refraction of the lens material.

Referring to the derivation of the transfer function, several points for the parabolic mirror as a system element can be made. First, since the focal length f of a mirror is not a function of index of refraction, the parabolic mirror system will not have the chromatic aberration that is inherent in the lens system.

Secondly all the light rays parallel to the z-axis will intersect the point f for a parabolic mirror, while only the paraxial rays will intersect the focal point for a spherical lens. This means that the parabolic mirror is inherently free from spherical aberrations (while the lens, of course, is not).

The absence of paraxial approximation for mirrors has several practical advantages, such as, that the aperture of the optical signal being processed can be larger for a parabolic mirror than for a lens of the same diameter. More importantly, it means that one can cut out off-axis segments from a parabolic mirror, and these segments will have the same transforming properties of the original mirror and the same relative axis. Thus one can construct folded optical processing system.

Two other aberrations also deserve some attention. Let us consider astigmatism. This aberration arises when the incoming light rays make a large angle with the z-axis of a mirror. This is not a serious drawback, however, since for most optical signal processing, the incoming light is a coherent plane wave whose rays are parallel to z-axis. Furthermore all interelement light paths can be kept at very small angles with respect to the element axes. Astigmatism therefore, can be made negligible in a parabolic processing system.

The second aberration is coma, the aberration that occurs for light rays at small angles to the Z-axis. In experiments using parabolic mirrors as Fourier transforming elements, the effects of coma were not observable at the normal working angles.

Figure 3 illustrates the optical data processing system using paraboloidal mirror segments. The coherent light source 1 is a p-n Gallium Arsenide laser with an effective radiating area of 3 mils. The laser operates at room temperature at a wavelength of 9000Å. It is placed in the focal plane of the paraboloidal mirror 3. The coherent monochromatic light 2 from GaAs laser diverges and typically forms a 30° angle. The coherent light sources is almost a point source and since it is in the focal plane of the paraboloidal mirror 3, the light reflecting from the paraboloidal mirror segment 4 is collimated.

To perform a two-dimensional spectrum analysis, the information to be analyzed is recorded on a transparency (either by taking the photograph or by electronically generating the object image). The transparency 6 is placed in the collimated beam 5 and is a focal length away from the paraboloidal mirror 7. The paraboloidal mirror segment converts the information of transparency 6 into a diffraction pattern that has all the properties of Fourier transform in the plane 10 centered at the point 9 which is the focal point of the paraboloidal mirror 7. The information in diffraction pattern can be converted into electrical signals by placing an appropriate photon detector 11 in the plane 10. The photon detector 11 could be of any suitable geometey such as in the form of wedges or concentric rings.

Spatial filtering can be performed in the plane 10. For example, the two basic type of filtering, "band pass" and "band stop" can be performed by having a transparent or an opaque region at a desired place in the plane 10. Optical filters in the form of wedges, annular ring or opaque disks were used in the plane 10. The light transmitting through the filter/detector 11 is reflected by a paraboloidal mirror segment 13 of paraboloid 14 placed a focal length away from the plane 10. The input information is reconstructed at the plane 15 which is a focal length away from the paraboloidal mirror 14.

Figure 4 shows the actual system and it can be seen that it can be housed with 6" × 3 1/2" × 1 1/2" space.

Experimental performance of the paraboloidal mirror segment system was evaluated by first monitoring the Fourier transform relationship in the focal plane of the mirror segment. As an example of single simple shapes Figure 5 shows the Fourier transform of a circular, rectangular and a triangular aperture. The well known Airy disk can be seen distinctly in the center of the transform of the circular aperture. Figure 5 also illustrates the example of multiple simple shapes. (A He-Ne laser was used for these experiments).

Figure 6 shows an example of spatial filtering. The Fourier transform of a triangle and its reconstructed image are shown in Figure 6(a). To filter out one of the sides of the triangle a narrow wedge was placed in the Fourier transform plane so that one of the components of the Fourier transform can be blocked. This and the effect of blocking the Fourier component is shown in Figure 6(b). It can be seen that the reconstructed image is without one side.

The missing side has been filtered or more correctly suppressed in the Fourier transform plane.

Figure 7 shows another example of spatial filtering. In this experiment a He-Ne gas laser was used as a source of coherent radiation mainly because the resolution of the image converter tube used in the image reconstruction plane was very low. A wire grid as shown in Figure 7(a) was chosen as an object. The Fourier transform of this object is shown in Figure 7(b). For spatial filtering purposes a slit was placed in the Fourier transform plane so that only the vertical structure of the Fourier transform was allowed to pass through the Fourier transform plane. The reconstructed filtered image is shown in Figure 7(c) and is without any vertical information. Figure 7(d) shows the reconstructed image without any spatial filtering.

Optical correlation experiments using paraboloidal mirror segments were also performed. Figure 8 illustrates the optical correlator. The input transparency was placed in the input plane. A Fourier transform hologram was recorded in complex spatial filter plane. The photographic film was developed and placed back exactly the same place it occupied during the exposure. The reference beam was blocked and the hologram was illuminated by the signal beam only.

Another off-axis paraboloidal mirror segment was used to Fourier transform the field transmitted by the hologram. The correlation plane which is located a focal length away from the off-axis mirror segment displays the convolution, geometrical image and correlation function. The auto correlation has a bright central peak that can be detected. Figure 9 shows such an example. The geometrical image of the input transparency and bright central peak of the auto correlation function can be easily seen.

A computer aided optical correlator system is under development, and is shown in Figure 10. The correlation spot is monitored by an image dissector tube. The output of this tube is interfaced with an IBM 1800 computer which controls the physical position of the input information. The correlation spot can be brought to a desired point by manuplating the position of the input information.

In conclusion the results obtained so far have shown that a low power, rugged and physically small optical system, capable of on-board spacecraft data processing can be constructed using off-axis paraboloidal mirror segments.

ACKNOWLEDGMENT

The author would like to thank Mr. David H. Schaefer for his encouragement in preparing this paper.

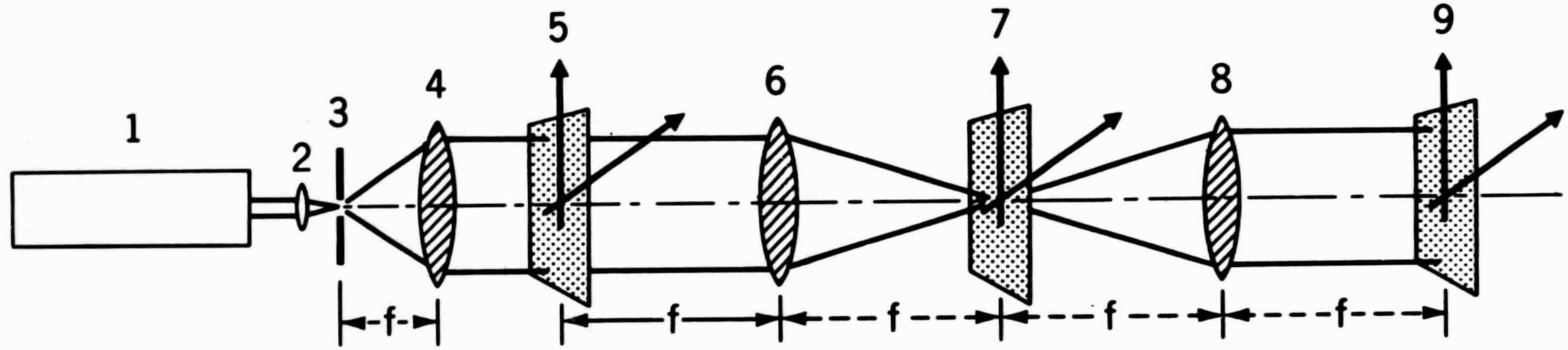

1. He–Ne GAS LASER
2. MICROSCOPIC LENS
3. PIN HOLE
4. COLLIMATING LENS
5. INPUT PLANE
6. FOURIER TRANSFORMING LENS
7. FOURIER TRANSFORM PLANE
8. IMAGE RECONSTRUCTING LENS
9. IMAGE RECONSTRUCTION PLANE

Figure 1. The Conventional Optical Data Processing System

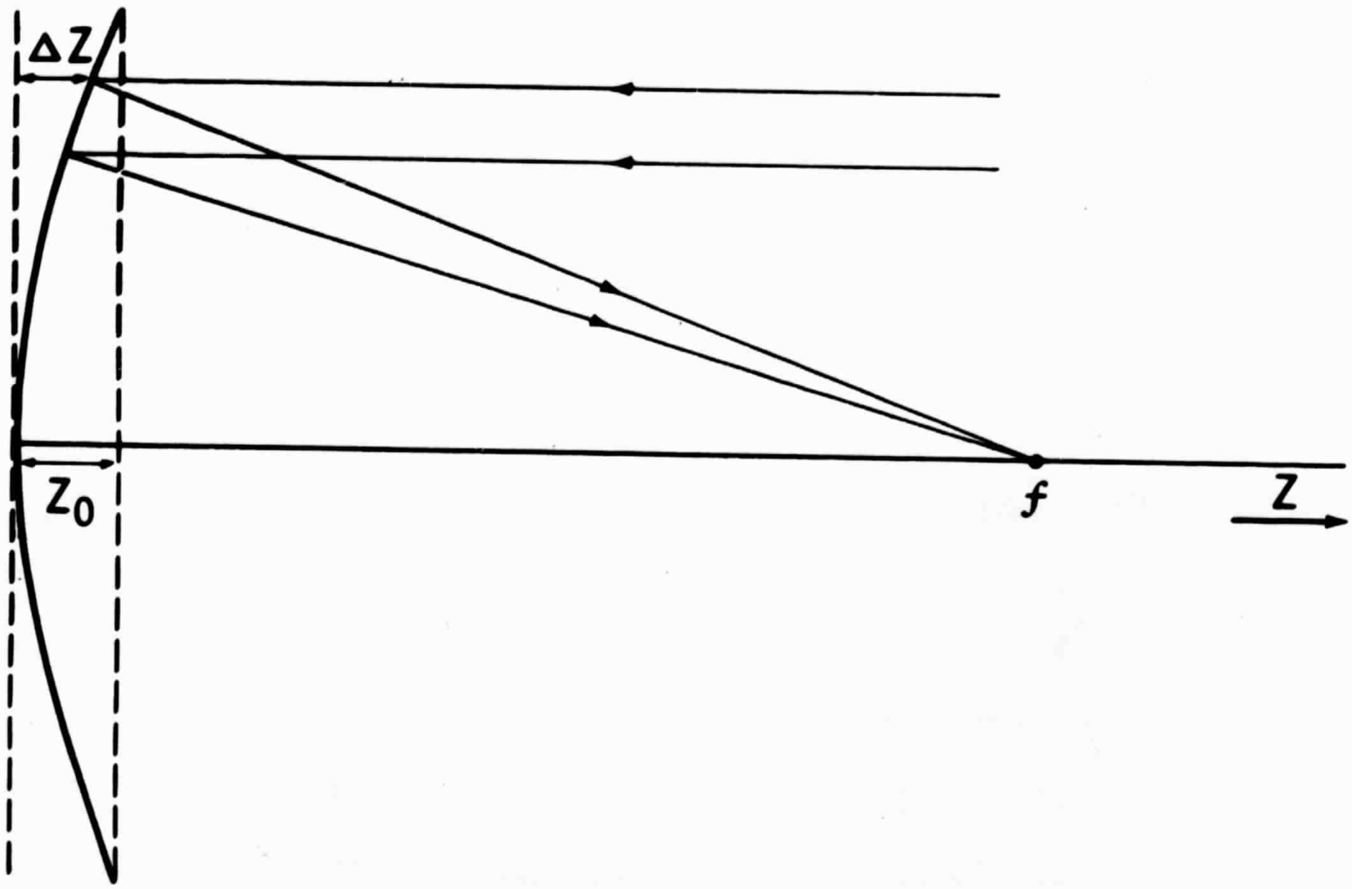

Figure 2. Transfer Function for Parabolic Mirror

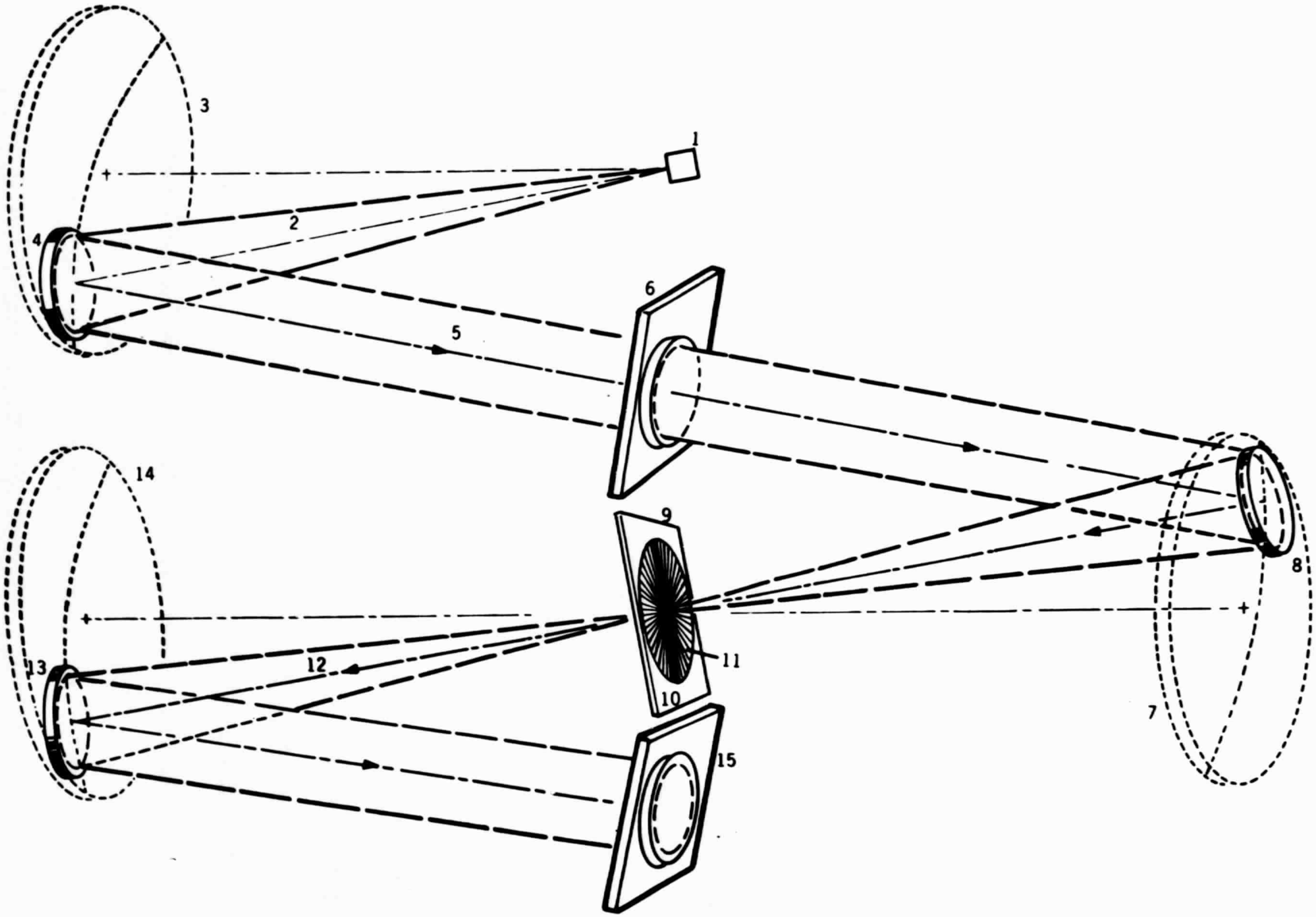

Figure 3. Optical Data Processor

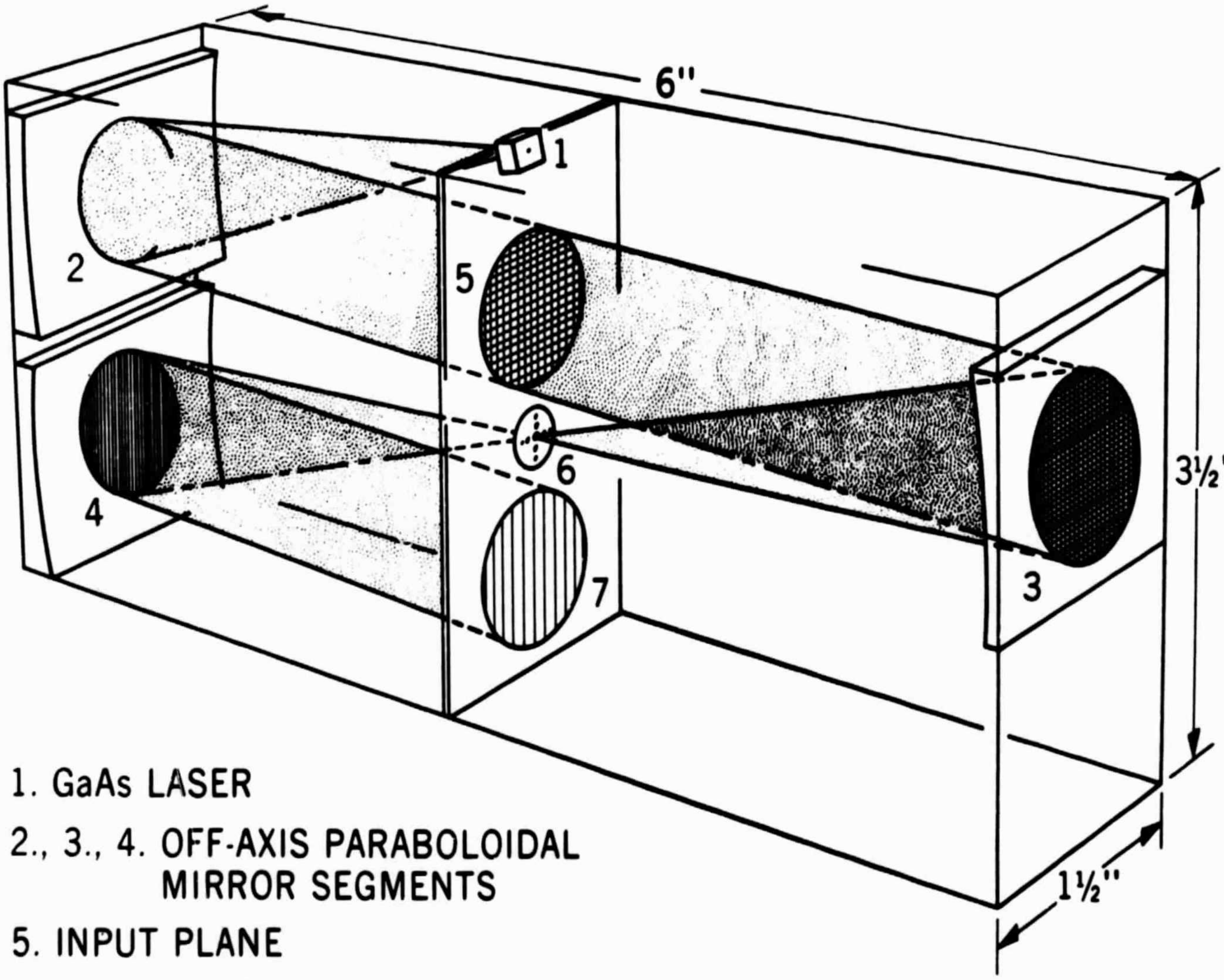

Figure 4. A Conceptual Design of the Optical System

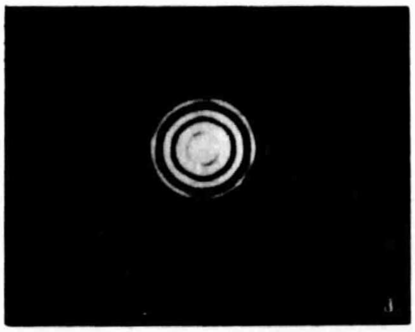

FOURIER TRANSFORM OF A CIRCULAR APERTURE

FOURIER TRANSFORM OF A RECTANGULAR APERTURE

FOURIER TRANSFORM OF A TRIANGLE

THE OBJECT TRANSPARENCY

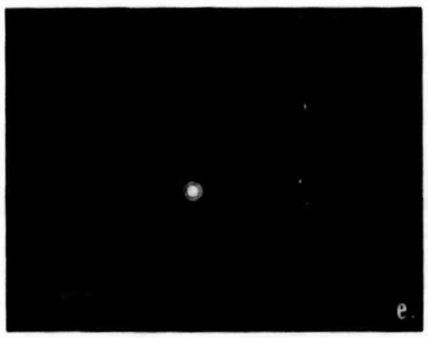

FOURIER TRANSFORM (d)

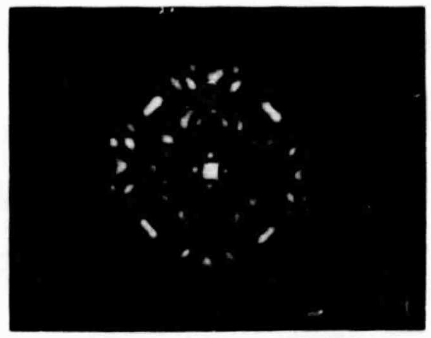

ENLARGED VIEW OF CENTRAL PORTION OF (e)

Figure 5. Experimental Performance of Paraboloidal Mirror Segments as a Fourier Transforming Element

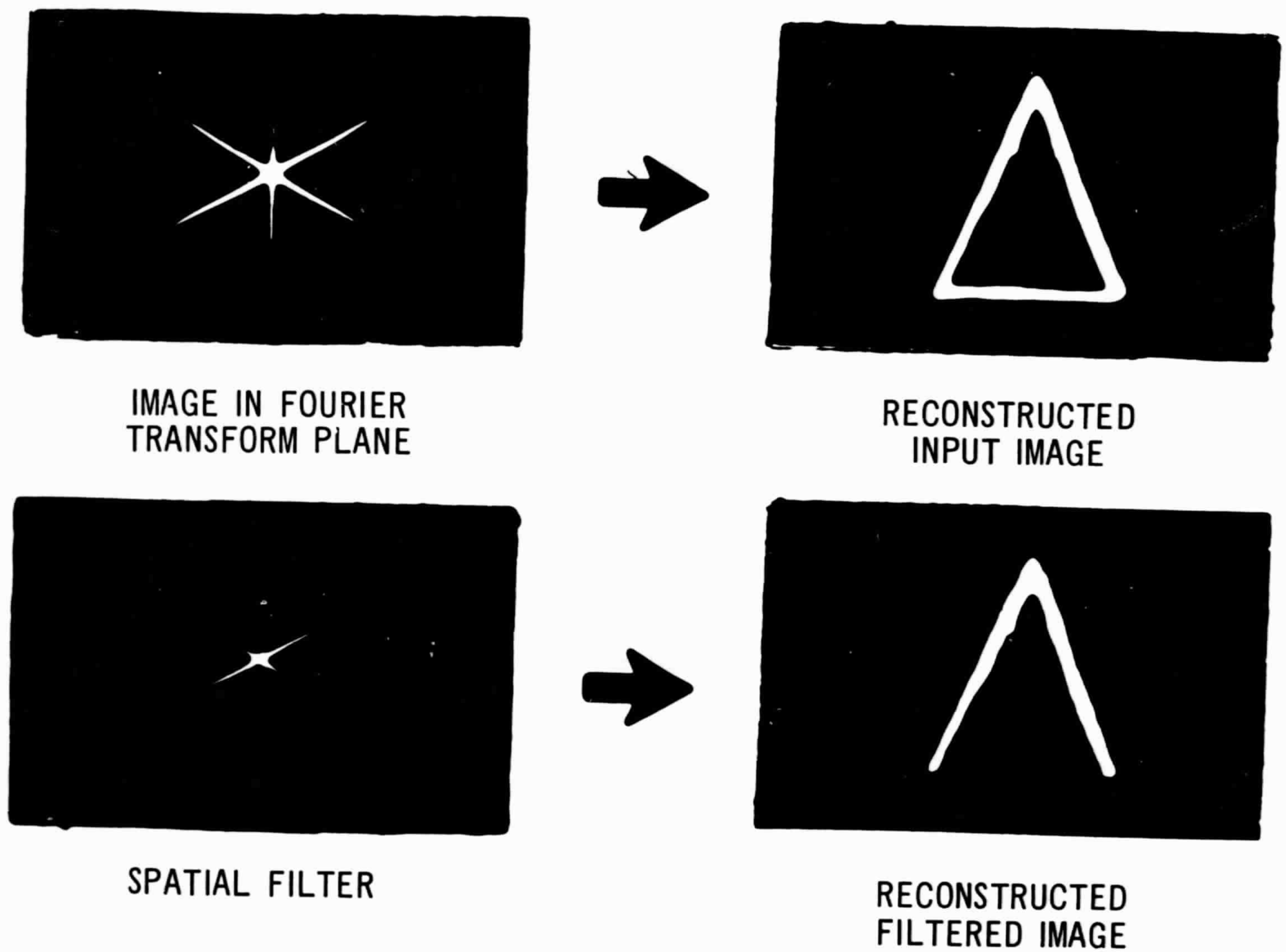

Figure 6. Coherent Optical Processing Using Gallium Arsenide Laser Source

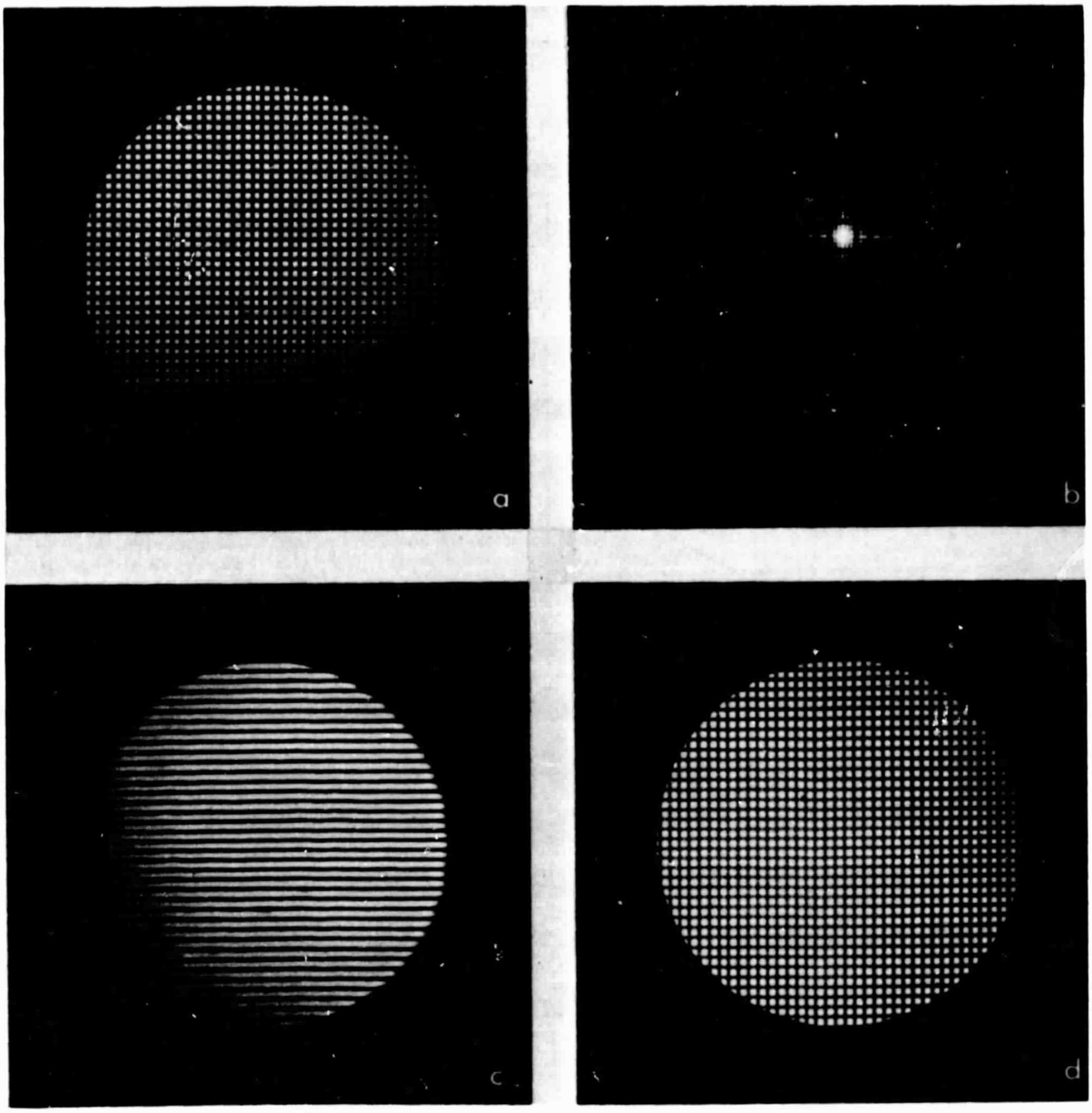

Figure 7. Spatial Filtering Experiment
(a) A Wire Grid in a Circular Aperture (The Object Transparency)
(b) Fourier Transform of (a)
(c) The Filtered Reconstructed Image
(d) The Unfiltered Reconstructed Image

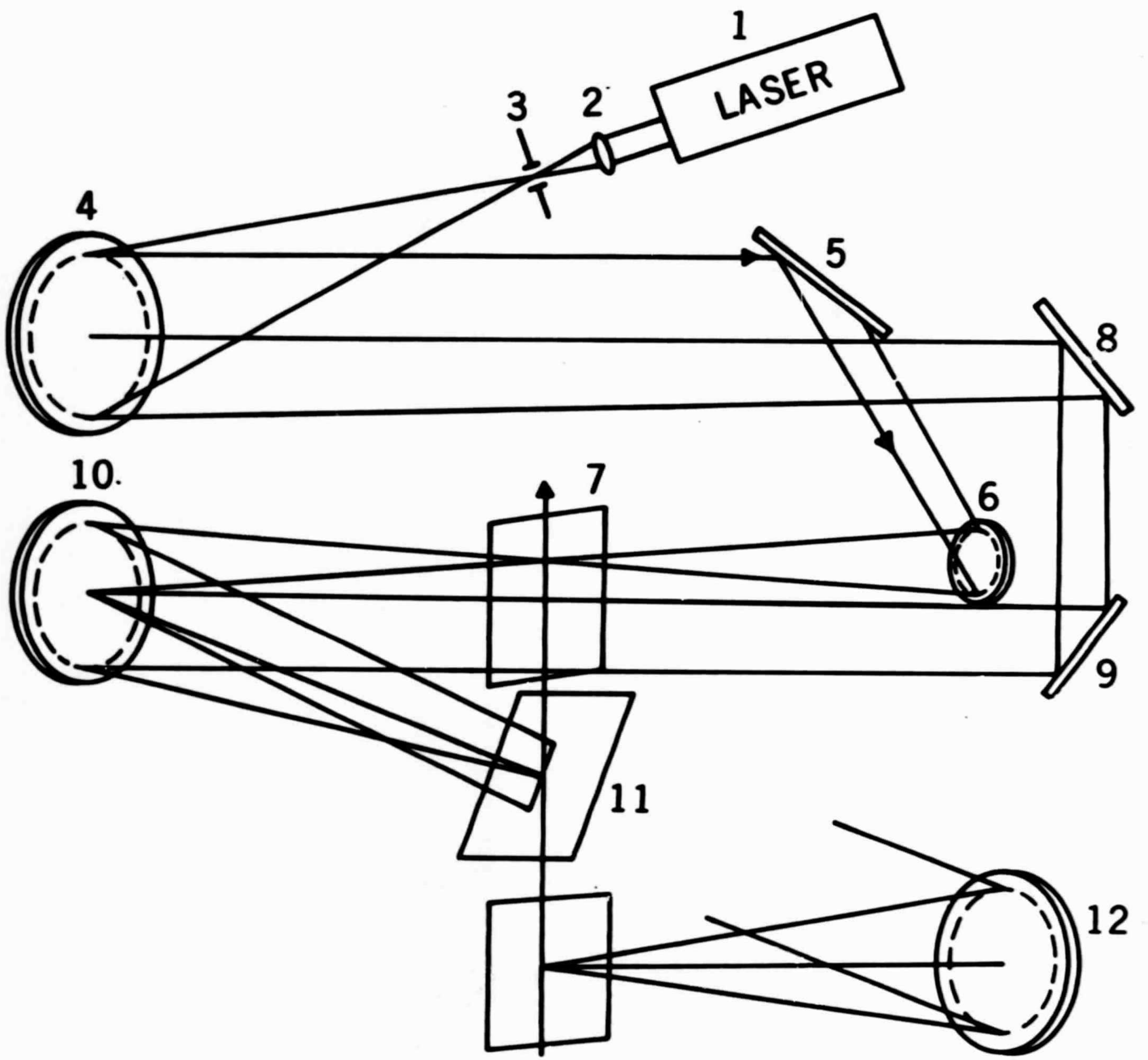

1. He-Ne LASER
2. MICROSCOPE LENS
3. 6 MICRON PIN HOLE
4. COLLIMATING PARABOLIC MIRROR
5. FRONT SURFACE MIRROR
6. FOCUSING PARABOLIC MIRROR (OFF AXIS SEGMENT)
7. INPUT PLANE
8. FRONT SURFACE MIRROR
9. FRONT SURFACE MIRROR
10. OFF-AXIS PARABOLOIDAL MIRROR SEGMENT FOR FOURIER TRANSFORMING
11. COMPLEX SPATIAL FILTER PLANE
12. OFF-AXIS PARABOLOIDAL MIRROR SEGMENT FOR FOURIER TRANSFORMING
13. CORRELATION PLANE

Figure 8. Optical Correlator Using Paraboloidal Mirror Segments

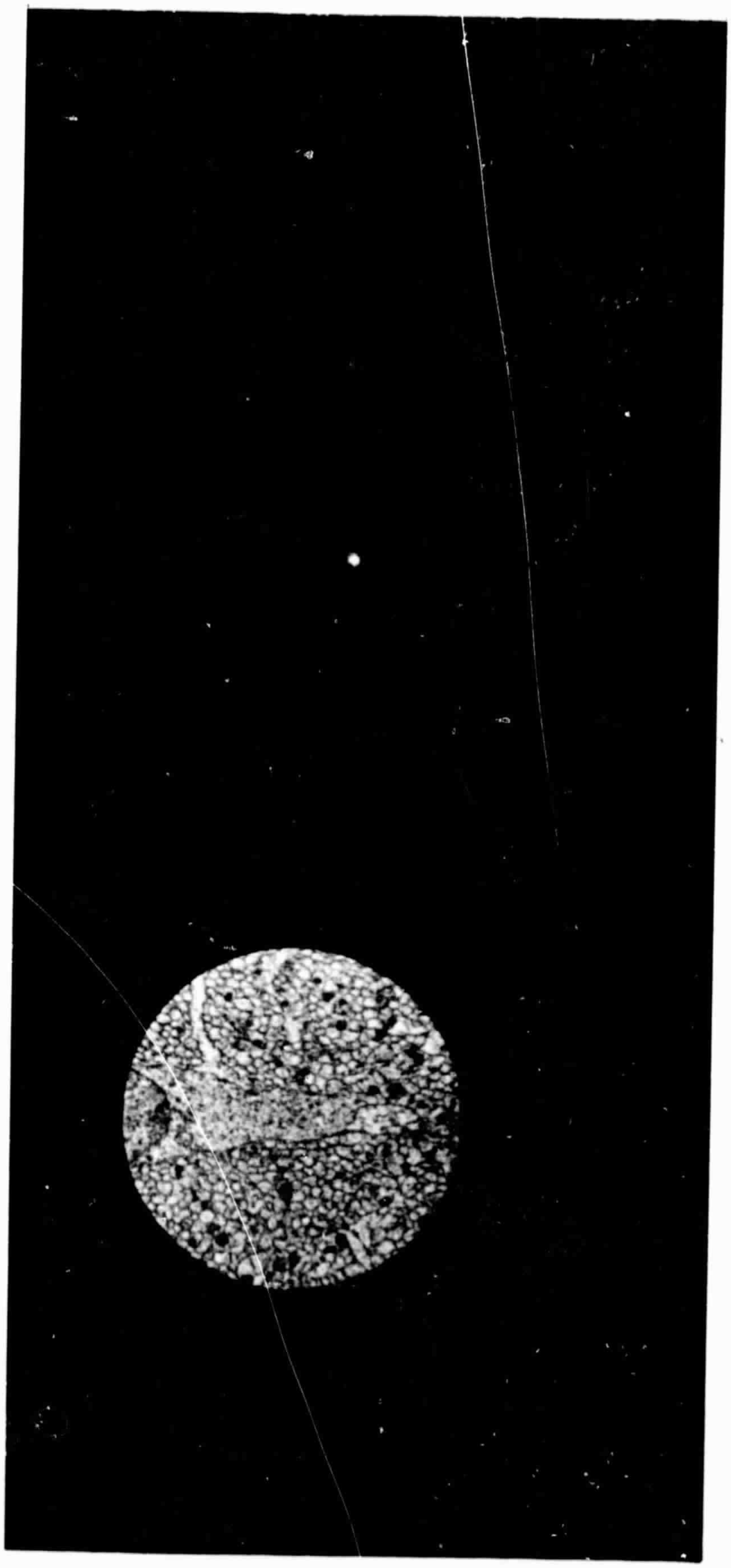

Figure 9. Optical Correlation Experiment

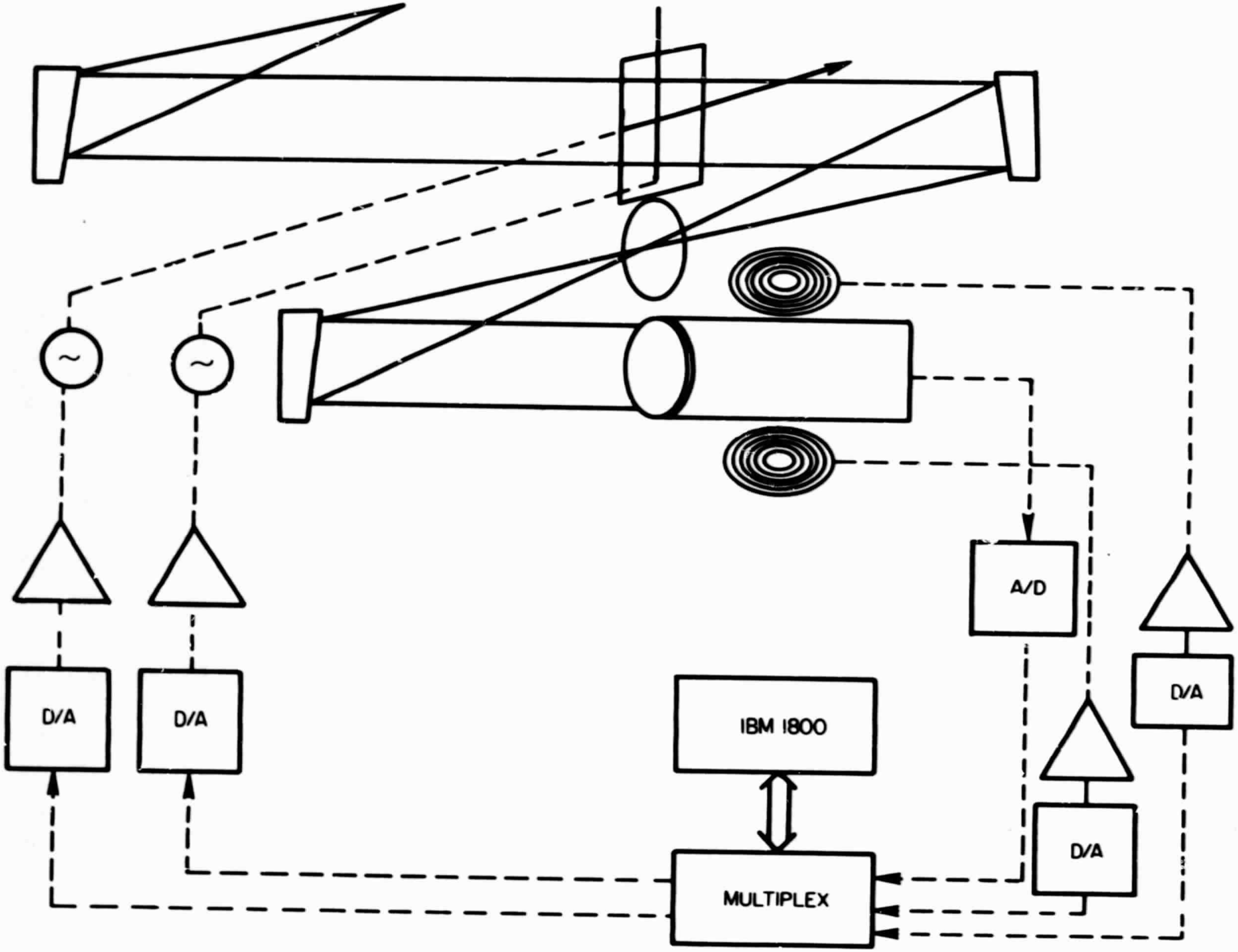

Figure 10. An Automatic Optical Correlator